Effect of Temperature on Unlubricated Sliding Wear of Additively Manufactured Stainless Steels

Junhyun Kwon*, Jung-Min Kim, Hyung-Ha Jin
Materials Safety Technology Development Division, Korea Atomic Energy Research Institute, Daejeon, 34057, KOREA
**Corresponding author: jhkwon@kaeri.re.kr*

1. Introduction

In nuclear power plants (NPP), tribological problems can occur to some components that are subject to relative motions such as those in the control assembly, the reactors and the steam generators. Due to a combination of impact and sliding motion, wear of components can take place. Wear is a surface damage involving a complex process that is affected by the physical, mechanical and chemical characteristics of elements, the medium and the environments [1]. Cases of wear have been observed on NPP parts, which include the rod cluster control assembly (RCCA) and the control rod drive mechanism latch arms in the French NPPs [2]. Also, similar damage of the RCCA components happened to the US NPPs [3]. Since those components are critical to the reactor safety, it is necessary to replace the damaged parts with new ones in a timely manner.

Recently, additive manufacturing (AM) technology has been drawing interest in a nuclear industry. There are a number of potential applications for AM, including replacement parts for operating reactors and structural prototypes for next generation nuclear systems. Austenitic stainless steel (SS) is widely used for components both inside and outside the reactor coolant pressure boundary. In this study, considering tribological problems that may happen to NPP parts, we investigate wear properties of AM SS 304L, which was made by the powder bed fusion (PBF) and the directed-energy deposition (DED) methods. Based on the pin-on-disk test results at two temperatures of 25 and 250ºC [4], the effect of temperature on the wear mechanism is examined for AM SS.

2. Experimental Procedure

2.1 Materials Processing

Two kinds of AM 304L specimens were produced by the PBF and DED method. Spherical 304L SS powder with different size was used as a feedstock. In the PBF process, an average particle size is between 15 to 45 μm in diameter and the density of the powder is 3.97 g/cm^3, which was provided by ChangSung Corporation (Korea). The specimen was fabricated using a commercial PBF equipment, Laser CUSING (Concept Laser, US). A fiber laser beam with a power of 180 W is directed with a scan speed of up to 800 mm/s across the deposited powder layer. The PBF process is carried out in a closed process chamber in which an inert gas is continuously maintained, so the residual oxygen content is kept to be less than 0.5 %.

We used 304L SS powder provided by CARPENTER (US) in the DED process, which has a particle size of 45 to 150 μm in diameter and the density of 4.34 g/cm^3. The DED system MX-400 (InssTek, Korea) equipped with an Nd:YAG fiber laser is used to manufacture the sample. The DED process parameters are set as follows: laser power 400 to 500 W, hatch spacing 0.5 mm, layer thickness 0.25 mm and scan speed 14 mm/s. Both PBF and DED samples were built in a rectangular bar with size of 125 x 60 x 30 mm.

2.2 Hardness Test

Hardness measurements for the AM 304L SS samples were performed using a micro-hardness tester (HM-122, Akashi) with a load of 1 kgf. We measure the hardness on a face parallel to the building direction at regular intervals upward from the baseplate and compare them with that of wrought 304L SS.

2.3 Pin-on-Disk Wear Test

The unlubricated sliding wear tests on 304L SS were carried out according to the ASTM standard G99, which is titled as 'Standard test method for wear testing with a pin-on-disk apparatus' [4]. The test rig consists of a vertical pin, 5 mm in diameter, which is loaded against a horizontal rotating disk, 30 mm in diameter. The wear test parameters were as follows: 30 N of normal load, sliding velocity of 0.22 m/s and total sliding distance of 1600 m. The wear tests were performed at 25 and 250ºC to investigate the temperature effect on wear properties. The degree of wear was determined by measuring the weight loss of specimens before and after the test, which was finally converted to the changes in volume.

3. Results

3.1 Hardness Measurement

The measured Vickers hardness data for 304L SS specimens were listed in Table I. The hardness values of the AM samples were obtained by averaging a number of measurements. The hardness for two AM specimens was higher than that for wrought SS and the DED sample has highest hardness among the specimens.

Table I: Vickers hardness measurement of 304L SS samples (wrought, PBF, DED)

Hardness	wrought	PBF	DED
Vickers (HV)	152	218.9 ± 2.5	247.7 ± 5.3
SI unit (MPa)	1491	2147 ± 25	2430 ± 52

3.2 Wear Properties

The amount of wear was determined by measuring the difference in the weight of specimens before and after a sliding test. Since test results are commonly reported as the wear rate in the unit of volume loss per unit distance slid, the measured weight loss was converted to the wear rate. The wear rates for three kinds of samples (wrought, PBF, DED) at 25 and 250°C are expressed in Fig. 1. At room temperature, the DED sample displays the highest wear resistance, implying the lowest wear rate. This finding is in agreement with the Archard wear equation [5], in which the wear resistance is directly related to the hardness of the material.

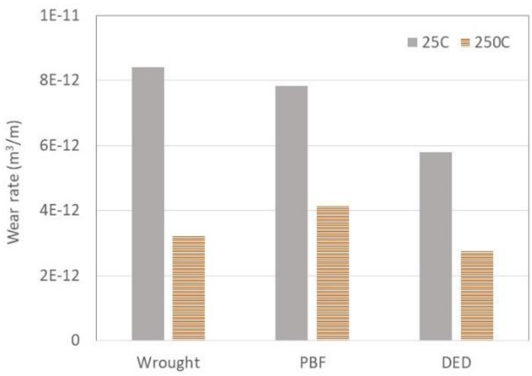

Fig. 1. Wear rates for 304L SS samples (wrought, PBF, DED) at 25 and 250°C

It is also found that the wear rate for all samples diminished significantly at high temperature. The relationship between the hardness and wear rate was not identified for the wear test at 250°C. A drop in wear rate is associated with change in the wear mechanism. While bright metallic surface was seen for disk samples tested at 25°C, we could observe a thin layer of dark oxide film distributed sporadically over the wear surface on the high-temperature disks. The appearance of wear surface for the RT and high-temperature sample is presented in Fig. 2. As the oxide film that was created at high temperature prevents direct metallic contact, it affects a decrease in the wear rate.

Fig. 2. Appearance of disk surface of 304L SS samples after pin-on-disk test at 25°C (left) and 250°C (right)

4. Discussion

The unlubricated (dry) wear behavior of additively manufactured 304L SS was investigated. At room temperature, the DED sample with the highest hardness exhibits strong wear resistance. This follows the Archard's law which is given by [5]:

$$W = \frac{k_A F}{H} \quad (1)$$

where W is the wear rate, F is the normal load, H is the hardness of the softer material and k_A is the Archard wear coefficient (dimensionless, typically ranging 10^{-5}~10^{-3}). At sliding velocities below about 0.1 m/s, the surface heating is negligible. In this case, shearing of successive surface layers causes plastic failure. In this regime, the wear rate tends to follow the Archard's law. As seen from Fig. 2, the wear surface obtained from room-temperature test at the speed of 0.22 m/s shows the bright metallic character, implying the plasticity-dominated wear is prevalent.

When the sliding speed is smaller than 1 m/s, the low speed does not generate a high flash temperature enough to oxidize the surface. In this study, however, dark oxide film was observed on the wear surface from the high-temperature test, which can be verified visually in Fig. 2. It is highly probable that the test temperature causes the oxidational-wear. To investigate the wear mechanism systematically, we applied the wear map for steel that was constructed by Lim and Ashby [6]. Fig. 3. exhibits the wear-mode map which depicts the various regions in which different modes of wear dominate as a function of normalized pressure and velocity. The black thick lines represent the field boundaries along which two wear modes can take place at an equal rate. Superimposed on the wear map are wear rates that we obtained from the pin-on-disk test for AM 304L SS. Though regardless of temperature all data belong to delamination-wear region

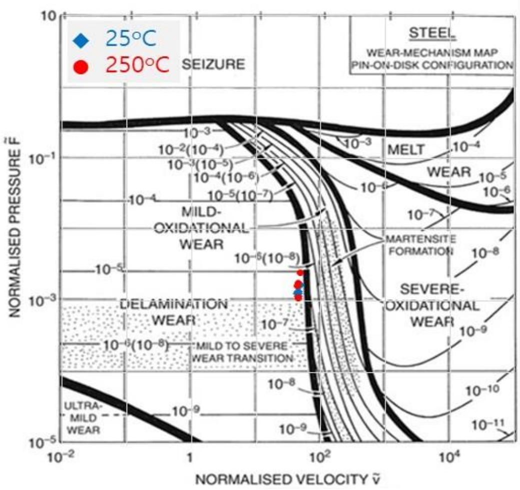

Fig. 3. Superimposition of the test results onto the wear-mode map for steel [6] (blue from 25°C test, red from 250°C)

(plasticity-dominated wear), they are located close to boundaries between plasticity-dominated and mild-oxidational wear. It is believed that the test temperature affects the wear mechanism by shifting from plasticity-dominated to oxidational-wear.

5. Conclusions

In a nuclear industry, it is challenging to apply the AM products to a nuclear system. Whereas AM materials have achieved a significant success with reasonable microstructure and suitable tensile properties, most work has focused on the fundamental characterization of AM materials. In this study, the wear properties of AM 304L SS were evaluated using a pin-on-disk test for the application of reactor components. From this work, the following facts can be found.

(1) At room temperature, the DED samples shows better wear resistance than wrought and PBF ones, which is related to the high value of hardness. This funding is in agreement with the Archard's law.

(2) At high temperature, the wear rates for all samples diminished significantly. Judging from residual surface oxides on the disk specimen after test, oxidation affects the wear mechanism. From the wear-mode map, it can be inferred that the dominant wear mechanism shifts from plasticity-dominated to mild oxidational-wear.

REFERENCES

[1] P.L. Ko, Wear of power plant components due to impact and sliding, *App. Mech. Rev.*, Vol.50, No.7, p.387, 1997.
[2] D. Hertz, Approach to analysis of wear mechanisms in the case of RCCAs and CRDM latch arms: From observation to understanding, *Wear* 261, p.1024, 2006.
[3] C. Wax, 2018 Materials programs technical information exchange meeting guide card wear update, PWR Owners Group, May 2018, Washington DC, US.
[4] Standard test method for wear testing with a pin-on-disk apparatus - ASTM G99-17, ASTM international, 2017, PA, US.
[5] I. Hutchings and P. Shipway, Tribology: Fraction and Wear of Engineering Materials, 2nd ed., B-H Publishing, 2017.
[6] S.C. Lim, M.F. Ashby, Wear-mechanism maps, *Acta metall.* Vol.35, No.1, p.1, 1987.